Turning SrTiO₃ into a Mott insulator

L. Bjaalie, A. Janotti, B. Himmetoglu, and C. G. Van de Walle

Materials Department, University of California, Santa Barbara, California 93106-5050, USA

SrTiO₃ (STO) is at the core of recent discoveries of two-dimensional electron gas (2DEG) formation at complex oxide interfaces, with the 2DEG residing on the STO side. Experimental results for ultrathin STO layers inserted in GdTiO₃ reveal a transition from metallic to insulating behavior, and suggest a strong interplay between electron-electron interaction and lattice distortions. Using first-principles calculations, we show that the metal-to-insulator transition is a bulk property of STO that emerges at extreme doping levels. We find that doping with 1/4 electron per Ti atom produces a metallic phase as expected, but that adding 1/2 electron per Ti results in a charge-ordered Mott-insulating phase. The effects of electron-electron interactions and lattice distortions are disentangled, and the Mott-insulator phase is shown to occur in STO/LaAlO₃ and STO/GdTiO₃ heterostructures with ultrathin STO layers.

SrTiO₃ (STO) is a band insulator, stable in a cubic perovskite crystal structure (5-atom unit cell) at ambient temperature. It often serves as a substrate for the growth of other materials [1]. Its indirect band gap of 3.2 eV separates the occupied valence band, formed by O $2p$ orbitals, from an empty conduction band formed by Ti $3d$ orbitals with t_{2g} symmetry [2]. Controlled n-type doping in bulk or in thin films can be achieved by replacing Ti with Nb atoms [3] or Sr with La atoms [4–6], leading to electrons occupying the conduction band with densities up to 7×10^{21} cm^{-3} (0.4 electron per Ti site), and a small, yet detectable, increase in lattice parameters [3,4]. These carrier densities are higher than those achieved in conventional semiconductors. Doping can also spontaneously occur in heterostructures such as STO/LaAlO₃ (LAO) [7,8] or STO/GdTiO₃ (GTO) [9], where a two-dimensional electron gas (2DEG) forms on the STO side due to the polar discontinuity at the interface [10]. Along the [001] direction, STO is composed of neutral SrO and TiO₂ planes, whereas GTO, for example, is composed of charged (GdO)⁺ and (TiO₂)⁻ planes. At the interface, excess electrons are transferred from the GdO plane to the STO conduction band, forming a 2DEG with 1/2 electron per unit-cell area [9,11].

In this work, we use density functional theory (DFT) with a hybrid functional to show that STO can drastically change its behavior when doped at very high levels. Rather than behaving as a heavily doped semiconductor, a charge-ordered Mott-insulating state emerges when 1/2 electron per Ti atom is added to STO, with an occupied lower Hubbard band (LHB) separated by an energy gap from an unoccupied upper Hubbard band (UHB), both derived from Ti $3d$ states. This Mott-insulating state is characterized by a large distortion of the crystal structure, with Ti-O-Ti angles of 165°, compared to 180° in the perfect cubic phase. Such extreme electron concentrations can probably not be induced by conventional doping, but they can be achieved by polar discontinuity doping at heterojunctions, where each interface contributes 1/2 electron per unit-cell area. We show that if the resulting electron gas is confined within a single STO layer (embedded in either GTO or LAO), the Mott-insulating state arises. Recent experiments on GTO with a single embedded STO layer

have indeed found evidence of an insulating state [12], with structural distortions in the STO layer [13].

Our calculations are based on generalized Kohn-Sham theory [14,15] within the projector-augmented wave method as implemented in the VASP code [16–18]. In order to simulate Mott-insulating behavior, which results from strong electronic correlation, we use the hybrid functional of Heyd, Scuseria, and Ernzerhof (HSE) [19]. This functional has been shown to yield an accurate description of electron localization [19], which makes it appropriate for simulating perovskite Mott insulators [20]. In the HSE functional, the exchange and correlation potential is divided into long- and short-range parts. Nonlocal Hartree-Fock exchange is mixed with the semilocal exchange of Perdew, Burke, and Ernzerhof [21] (PBE) in the short-range part, while the correlation and the long-range part of the exchange potential are described by PBE. The mixing parameter and the inverse screening length were set to the standard values of 0.25 and 0.1 Å^{-1}.

For STO we use a $\sqrt{2} \times \sqrt{2} \times 2$ supercell with a $6 \times 6 \times 2$ special k-point mesh for integrations over the Brillouin zone and an energy cutoff of 500 eV for the plane-wave basis set. The calculated lattice parameter of STO is 3.903 Å, and the indirect band gap (Γ-R) is 3.27 Å. For the heterostructures with thin STO layers, we considered (LAO)₂.₅/(STO)₁.₅ and (GTO)₂.₅/(STO)₁.₅ superlattices. These calculations were performed using a $4 \times 4 \times 1$ special k-point mesh, and all include spin polarization. Exchange splitting is indeed essential to split off singly occupied lower Hubbard bands—if there was no spin polarization, the bands would all be doubly degenerate. Spin-orbit coupling was not included; the resulting conduction-band splitting is only 28 meV in STO [22] and would not affect any of our results.

We first consider STO in a unit cell of 20 atoms (four SrTiO₃ formula units), to which we add one or two electrons and allow the volume and all the atomic positions to relax. Figure 1(a) shows the relaxed atomic structure and the corresponding conduction-band structure of a neutral 20-atom cell of STO. The crystal structure is very close to cubic, with lattice parameters of 5.520 Å (a, b) and 7.807 Å (c). Ti-O-Ti angles in this structure should be 180° (our choice of k-point mesh breaks the cubic symmetry and leads to inaccuracies on
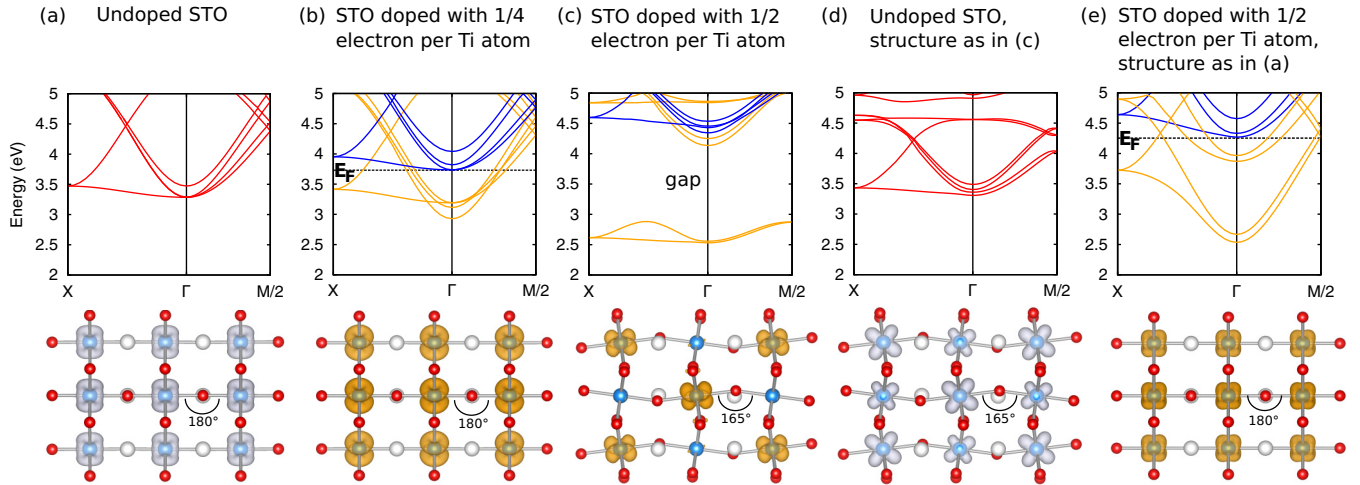
FIG. 1. (Color online) Evolution of electronic and atomic structure of STO as electrons are added. The conduction bands are plotted along the Γ-X and Γ-M/2 directions in the Brillouin zone (BZ) of the 5-atom cubic perovskite unit cell, which correspond to Γ-M and Γ-X in the BZ of the 20-atom cell. Red lines correspond to bands that are non-spin-polarized, orange to spin-up, and blue to spin-down bands. The top of the valence band is set as the reference. For the doped cells, the charge density of the occupied conduction-band states is shown (in orange) superimposed on the crystal structure, and for the undoped cells the charge density of the (unoccupied) lowest-lying conduction-band states at the Γ point (in gray) is shown. In all cases the isosurface is set to 10% of the maximum. Undoped STO is shown in (a), STO doped with 1/4 electrons per Ti in (b), and STO doped with 1/2 electrons per Ti in (c). In (d), the crystal structure is the same as in (c), but excess electrons are removed. In (e) the crystal structure is the same as in (a), but doped with 1/2 electrons per Ti.

the order of 0.5°). Due to the octahedral crystal field, the $3d$ orbitals of Ti are split into lower-energy triply degenerate states with t_{2g} symmetry, and higher-energy doubly degenerate states with e_g symmetry. The conduction band derived from the t_{2g} orbitals is triply degenerate at the Γ point. Adding electrons to STO leads to partial occupation of the t_{2g}-derived bands, and within band theory, a metallic behavior is expected.

Upon adding one electron to the 20-atom cell, corresponding to an excess electron density of 1/4 per Ti atom, and allowing the crystal structure to relax, we find that the system is metallic and remains in an almost perfectly cubic structure. The resulting band structure and the charge density corresponding to the partially filled conduction bands are shown in Fig. 1(b). The lattice parameters increase by 1.3% (a, b) and 1.2% (c) compared to undoped STO. The change in lattice parameters upon electron doping is in line with experimental results [3]. An additional feature that arises as a result of doping STO with 1/4 per Ti atom is strong exchange splitting within the conduction band.

Attempts to localize the extra electron on a particular Ti atom in the 20-atom cell by slightly displacing the surrounding O atoms to accommodate the extra charge were unsuccessful. We also performed calculations for a 135-atom supercell, again finding that an excess electron prefers to stay delocalized, with a charge distribution equally shared by all the Ti atoms.

For a doping level of 1/2 electron per Ti (i.e., adding two electrons to the 20-atom cell), the structure displays GdFeO$_3$-type distortions and a 1.26 eV gap opens within the t_{2g} derived bands, as shown in Fig. 1(c). The calculated density of states (not shown) confirms this result. The Ti-O-Ti angles decrease to 165° and 163°, and the lattice parameters increase by 2.6% (a, b) and 3.7% (c) compared to undoped STO. Based on the structural distortions we would expect a decrease in the lattice parameters; the observed increase is

attributed to the effect of electron addition [4]. The distortions break the cubic symmetry seen by the Ti atoms, leading to a splitting of degenerate Ti $3d$ t_{2g} states, with a corresponding change in the orbital character of the bands. This is illustrated for the lowest-lying conduction band at the Γ point for the undoped cubic and distorted cases in Figs. 1(a) and 1(d). It therefore becomes possible to split off a band derived from a single occupied orbital, which is what we observe upon electron addition: a LHB splits off, with each band derived from a single orbital (d_{xz} and d_{yz}) localized on a single Ti atom. Exchange splitting is also required to form the LHB, as it splits off the corresponding spin-down bands. We thus see the formation of a charge-ordered insulating ground state, with the added electrons residing on every other Ti atom in a three-dimensional checkerboard arrangement. In Fig. 1(c) the charge density of the added electrons is plotted. The insulating state exhibits a ferromagnetic order with the antiferromagnetic arrangement higher in energy by 5 meV per Ti atom.

We speculate that this Mott-insulating phase would be stable with respect to small deviations in the doping level, since phase separation is likely to occur. For a doping level below 1/2 electrons per Ti, a small fraction of the system would be undoped STO, also insulating. For doping levels above 1/2 electrons per Ti, a small fraction would be STO doped with 1 electron per Ti, which is insulating, with a distorted crystal structure (same situation as in, e.g., GTO). Unfortunately, explicit calculations investigating this behavior would require much larger supercells than computationally tractable.

In order to separate the effects of lattice distortions and electron-electron interactions, it is instructive to consider two test cases: (1) a distorted STO structure with the same atomic positions as in Fig. 1(c) but without the extra electrons; and (2) undistorted STO with the same structure as in Fig. 1(a) but

with doping of 1/2 electron per Ti atom. The band structure for the distorted but undoped case is shown in Fig. 1(d). Despite the large structural distortion, the conduction bands look remarkably similar to those in Fig. 1(a): degeneracies are split and avoided crossings occur, but no gap is observed.

The second case, where two electrons are added to the undistorted structure without allowing atomic relaxation, leads to a metallic state, as shown in Fig. 1(e). The conduction bands are partially occupied, leading to a metallic ground state, again with strong exchange splitting, but with no evidence of gap formation. These results provide powerful evidence that structural distortions are key to achieving the insulating state. In the absence of such distortions [case (2), Fig. 1(e)] the system remains metallic, even for the 1/2-electron-per-Ti case. Electron-electron interactions play a strong role as well, of course, evidenced by the significant differences in band structure between panels (c) and (d) of Fig. 1: structural distortions alone do not open up a gap, and electron localization is required to trigger gap formation. We conclude that *both* structural distortions and electron-electron interactions are *necessary* to trigger a metal-insulator transition, but neither is *sufficient* by itself.

The question then arises as to whether this insulating phase of highly doped STO may be observed in practice. In fact, such high doping levels are attainable in heterostructures with ultrathin STO layers, where each interface dopes the STO layer with 1/2 electron [10]. For instance, consider an LAO/STO/LAO heterostructure along the [001] direction, in which 1.5 unit cells of STO are sandwiched between two thicker LAO layers, with two equivalent and mirror-image LaO-TiO$_2$ interfaces, as shown in Fig. 2(a). Since the conduction band of LAO is significantly higher in energy than that of STO [11], it is expected that the excess electrons from the LaO plane at each interface (i.e, 1/2 electron per unit-cell area) are transferred to the STO conduction band [10], thus resulting in a total of two electrons per four Ti atoms in the STO layer, or 1/2 electron per Ti. According to our results for bulk STO, this exact filling would turn STO into a charge-ordered insulator, if the structure of the interface also accommodates distortions. With this picture in mind, we performed electronic structure calculations for an (STO)$_{1.5}$/(LAO)$_{2.5}$ superlattice containing two equivalent LaO-TiO$_2$ interfaces. The in-plane lattice parameter was fixed to that of STO (representing growth on an STO substrate), while the out-of-plane lattice parameter and all atomic positions were allowed to relax.

The band structure [Fig. 2(a)] shows that the heterostructure indeed displays insulating behavior, as conjectured. The highest two occupied bands, 2.8 eV above the bands derived from the O $2p$ orbitals, are identified as the STO LHB. The charge density corresponding to the LHB exhibits remarkable similarities to that of bulk STO doped with 1/2 electron per Ti [Fig. 1(c)]. Analogous to the bulk case, the ground state displays ferromagnetic order and the excess electrons are distributed on every other Ti site. The interfacial TiO$_2$ layers are distorted, with an out-of-plane Ti-O-Ti angle of 167.5°, only slightly larger than the angle in bulk STO doped with 1/2 electron per Ti (165°). For thicker STO interlayers, the three-dimensional density of electrons in the STO will be lower than 1/2 per Ti, and metallic rather than insulating behavior should be observed. Experimental results for LAO/STO/LAO
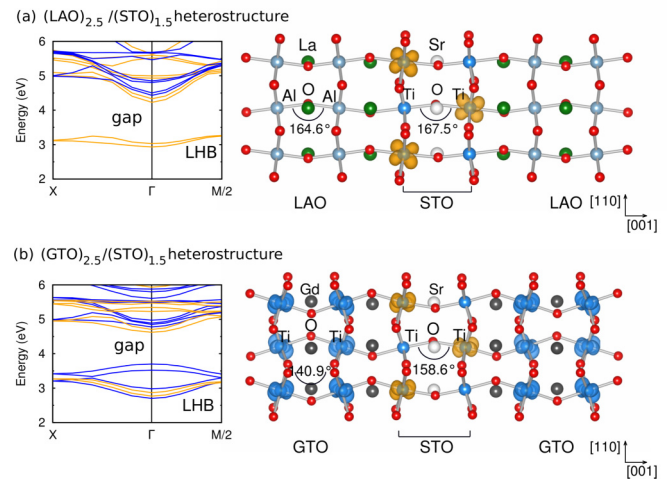
FIG. 2. (Color online) Electronic and atomic structure of LAO/STO and GTO/STO superlattices. The electronic band structures are plotted along the Γ-X and Γ-M/2 directions in the BZ of the 5-atom cubic perovskite unit cell, which correspond to the Γ-M and Γ-X directions in the 20-atom cell, and are perpendicular to the [001] growth direction. Orange lines correspond to spin-up, and blue to spin-down bands. The valence-band maximum is set as the energy reference. The results for (LAO)$_{2.5}$/(STO)$_{1.5}$ are shown in (a), and those for (GTO)$_{2.5}$/(STO)$_{1.5}$ in (b). The gap and the lower Hubbard bands are indicated in the band structures. Charge density plots are shown for the occupied lower Hubbard bands, and the isosurfaces were set to 10% of the maximum.

heterostructures with ultrathin STO layers and two equivalent LaO-TiO$_2$ interfaces have not been reported to our knowledge.

We also performed calculations for GTO/STO/GTO heterostructures, in the same manner as for LAO/STO. GTO itself is a Mott insulator, in which all Ti atoms occur in a 3+ oxidation state, with a LHB occupied by same-spin electrons and well separated from the UHB by a gap of 2.05 eV. For the purposes of the heterostructure, this Mott behavior is not of the essence, and GTO merely functions as a barrier layer, with the GdO-TiO$_2$ interfacial layers providing 1/2 electron per unit-cell area per interface to the STO conduction band [9].

Similar to (LAO)$_{2.5}$/(STO)$_{1.5}$, we carried out calculations for (GTO)$_{2.5}$/(STO)$_{1.5}$ superlattices [which in this case are identical to (GTO)$_3$/(STO)$_1$, since TiO$_2$ layers are common to both materials]. The electronic band structure [Fig. 2(b)] shows that this heterostructure is also insulating, with two (spin-up) bands in the LHB pertaining to the STO; the antiferromagnetic ordering of STO LHB electrons is higher in energy by 5 meV per Ti. Figure 2(b) shows four additional bands in the same energy region; these are the GTO LHBs (spin-down). We thus find that, again, the electrons contributed by polar-discontinuity doping from the GTO/STO interfaces trigger the formation of a charge-ordered insulating phase in the ultrathin STO layer. The distortions are again essential, with an out-of-plane Ti-O-Ti angle of 158.6°.

The GTO/STO/GTO heterostructure has also been investigated experimentally [12,23]. A 2DEG with nominal charge of 1/2 electron per unit-cell area per interface was observed [23]. As the STO layer becomes thinner, the number of electrons

per Ti in STO increases, and for a single SrO layer the system indeed transitions into an insulating state [12]. We also note that previous first-principles work was performed on this system, using DFT+U [24]. For the single SrO layer, an insulating ground state was interpreted as a Mott-dimer phase. Our results do not show evidence of dimerization and do not require it to explain the insulating state.

In summary, we have shown that doping with 1/2 electron per Ti can turn STO into a charge-ordered Mott insulator. Such extreme doping levels can be achieved in complex-oxide heterostructures. Our results explain recent experimental observations in ultrathin films of STO embedded in GTO. Predictions for the insulating state of TiO_2-SrO-TiO_2 embedded in LAO are yet to be confirmed. For device applications, it would be interesting if this Mott-insulating state could be transformed into a metallic state by electron or hole doping in a gated structure. A small change in the electron density could potentially lead to a transition to a metallic state, allowing conductivity changes of many orders of magnitude.

[1] G. Koren, A. Gupta, E. A. Giess, A. Segmüller, and R. B. Laibowitz, Appl. Phys. Lett. **54**, 1054 (1989).

[2] M. Cardona, Phys. Rev. **140**, A651 (1965).

[3] S. Ohta, T. Nomura, H. Ohta, M. Hirano, H. Hosono, and K. Koumoto, Appl. Phys. Lett. **87**, 092108 (2005).

[4] A. Janotti, B. Jalan, S. Stemmer, and C. G. Van de Walle, Appl. Phys. Lett. **100**, 262104 (2012).

[5] B. Jalan and S. Stemmer, Appl. Phys. Lett. **97**, 042106 (2010).

[6] T. A. Cain, A. P. Kajdos, and S. Stemmer, Appl. Phys. Lett. **102**, 182101 (2013).

[7] A. Ohtomo and H. Y. Hwang, Nature (London) **427**, 423 (2004).

[8] H. Y. Hwang Y. Iwasa, M. Kawasaki, B. Keimer, N. Nagaosa, and Y. Tokura, Nat. Mater. **11**, 103 (2012).

[9] P. Moetakef *et al.*, Appl. Phys. Lett. **99**, 232116 (2011).

[10] A. Janotti, L. Bjaalie, L. Gordon, and C. G. Van de Walle, Phys. Rev. B **86**, 241108(R) (2012).

[11] L. Bjaalie, B. Himmetoglu, L. Weston, A. Janotti, and C. G. Van de Walle, New J. Phys. **16**, 025005 (2014).

[12] D. G. Ouellette, P. Moetakef, T. A. Cain, J. Y. Zhang, S. Stemmer, D. Emin, and S. J. Allen, Sci. Rep. **3**, 3284 (2013).

[13] J. Y. Zhang, J. Hwang, S. Raghavan, and S. Stemmer, Phys. Rev. Lett. **110**, 256401 (2013).

[14] P. Hohenberg and W. Kohn, Phys. Rev. **136**, B864 (1964).

[15] W. Kohn and L. J. Sham, Phys. Rev. **140**, A1133 (1965).

[16] G. Kresse and J. Furthmüller, Phys. Rev. B **54**, 11169 (1996).

[17] G. Kresse and J. Furthmüller, Comput. Mater. Sci. **6**, 15 (1996).

[18] G. Kresse and D. Joubert, Phys. Rev. B **59**, 1758 (1999).

[19] J. Heyd, G. E. Scuseria, and M. J. Ernzerhof, J. Chem. Phys. **118**, 8207 (2003); **124**, 219906 (2006) [erratum].

[20] J. He and C. Franchini, Phys. Rev. B **86**, 235117 (2012).

[21] J. P. Perdew, K. Burke, and M. Ernzerhof, Phys. Rev. Lett. **77**, 3865 (1996).

[22] A. Janotti, D. Steiauf, and C. G. Van de Walle, Phys. Rev. B **84**, 201304(R) (2011).

[23] P. Moetakef, C. A. Jackson, J. Hwang, L. Balents, S. J. Allen, and S. Stemmer, Phys. Rev. B **86**, 201102(R) (2012).

[24] R. Chen, S. B. Lee, and L. Balents, Phys. Rev. B **87**, 161119(R) (2013).